Friction **12**(3): 375–395 (2024)
https://doi.org/10.1007/s40544-023-0751-9
ISSN 2223-7690
CN 10-1237/TH

REVIEW ARTICLE

Interactive mechanism and friction modelling of transient tribological phenomena in metal forming processes: A review

Xiao YANG[1,*], Heli LIU[1], Lemeng ZHANG[1], Yiran HU[1], Denis J. POLITIS[2], Mohammad M. GHARBI[3], Liliang WANG[1,*]

[1] *Department of Mechanical Engineering, Imperial College London, London SW7 2AZ, UK*

[2] *Department of Mechanical and Manufacturing Engineering, University of Cyprus, Nicosia 1678, Cyprus*

[3] *Quaker Houghton Deutschland GmbH, Dortmund 44319, Germany*

Received: 29 November 2022 / Revised: 09 February 2023 / Accepted: 26 February 2023

Abstract: The accurate representation of tribological boundary conditions at the tool–workpiece interface is crucial for analysis and optimization of formability, material flow, and surface quality of components during metal forming processes. It has been found that these tribological conditions vary spatially and historically with process parameters and contact conditions. These time-dependent tribological behaviours are also known as transient tribological phenomena, which are widely observed during forming processes and many other manufacturing application scenarios. However, constant friction values are usually assigned to represent complex and dynamic interfacial conditions, which would introduce deviations in the relevant predictions. In this paper, transient tribological phenomena and the contemporary understanding of the interaction between friction and wear are reviewed, and it has been found that these phenomena are induced by the transitions of friction mechanisms and highly dependent on complex loading conditions at the interface. Friction modelling techniques for transient behaviours for metal forming applications are also reviewed. To accurately describe the evolutionary friction values and corresponding wear during forming, the advanced interactive friction modelling has been established for different application scenarios, including lubricated condition, dry sliding condition (metal-on-metal contact), and coated system.

Keywords: transient tribological phenomena; interactive friction mechanism; modelling techniques; metal forming

1 Introduction

The challenging tribological conditions in metal forming processes, such as failure of formed components and limited tool-life, are always caused by severe contact conditions, poor lubrication, and mass/serial production during the forming of components with complex geometries and high strength materials. The tribological conditions are commonly evaluated by consideration of friction and wear during the forming process. Friction describes the tangential force generated at the contact point, which affects the material flow and drawability of the forming process. In comparison, wear occurs on both workpiece and tool and can cause damage to both surfaces, including material scratching, scoring, and galling, which can reduce tool-life and the surface quality of products.

Friction and wear are not material properties but two evolutionary variables of an identical tribo-system [1]. These variables are identified as the result of the combination of multiple influencing parameters, which can be classified into three categories: (1) material properties of the contact pair, (2) operation parameters, such as lubrication condition and surface roughness, and (3) contact parameters (or process variables), such as temperature, sliding speed, sliding distance,

* Corresponding authors: Xiao YANG, E-mail: x.yang17@imperial.ac.uk; Liliang WANG, E-mail: liliang.wang@imperial.ac.uk

contact pressure, and forming cycle. As friction and wear are simultaneously affected by the above-mentioned parameters, they are reasonably related to each other, and interactions are expected between these tribo-responses [1], which have resulted in the transient tribological phenomena. These transient phenomena have been observed in various interaction scenarios, including lubricant breakdown [2–4], adhesive wear (galling) [5, 6], coating breakdown [7, 8], oxide film [9], and reaction layer [10].

Lubricant breakdown is a form of lubrication failure where it is not possible to maintain completely hydrodynamic or mixed lubrication conditions at the contact interface. Moreover, there may be a considerable amount of boundary lubrication, during which wear of the surfaces may occur [11]. In metal forming processes, this lubrication failure is caused by lubricant layer uneven transportation and thinning during forming and may lead to lubrication starvation and direct contact/wear of the workpiece and tool. As opposed to mechanical systems such as bearing and gear, an adequate amount of lubricant applied before the initiation of the forming operation does not guarantee desirable lubricity through the entire forming process. Therefore, the term, lubricant breakdown, is adopted in the present work to distinguish the forming tribo-system from cyclic systems.

Galling is defined by the standard of American Society for Testing Material (ASTM) G40, as a form of macro-scale surface irregularities observed above the original interface. It usually features the formation of localized and rough protrusions, known as plastic flow or material transfer. Galling is more often mentioned in the industrial rather than the academic fields. For metal forming processes, galling is commonly referring to the severe adhesive wear and is characterized by the material transfer from the soft workpiece to the hard tool. In this process, a transfer layer is formed after repeated forming operations, especially at some critical positions, such as radii of a tool, which can result in high local friction, scratching on the workpiece and misalignment of a tool. Material transfer caused by adhesive wear may refer to other industrial terms, such as material pick-up, scuffing, localized welding, and seizing (seizure). Galling is the most widely used, and thus adopted in the present work.

Coating breakdown is caused by the abrasive and/or adhesive wear of a coated contact during the relative sliding process. The hard coating is usually applied on the metal forming tool due to its high hardness, good anti-galling resistance, and chemical stability. However, the coated tools, in these cases, experience severe impact, which includes both high interfacial temperatures and heavy cyclic loadings, which inevitably lead to damage and finally breakdown or failure of the tool. In addition, coating can also be applied on the workpiece as a source of solid lubrication [12]. In the coated system, there are four main influencing parameters that control the coating breakdown phenomenon, including the coating thickness, hardness ratio between the coating and the substrate, interfacial surface roughness, and the composition and hardness of wear particles [1, 13, 14].

Formation of oxide layers will lead to the transformation of friction mechanism at the contact interface, which is determined by the characteristics of oxides in frictional contact based on their tribological natures and interfacial temperatures, either abrasive or lubricious. With the increase of interfacial temperature, the decrease of coefficient of friction (COF, μ) is probably due to the formation of oxides and/or intermetallic compounds, which would consequently reduce adhesion. On the other hand, the principal wear mechanism is the combination of adhesive wear and the contributions from abrasion of oxidized wear debris at elevated temperatures [12, 15, 16].

The transient tribological phenomena are also found to be highly affected by the instantaneous contact conditions such as interfacial temperature, pressure, and relative sliding speed at the tool–workpiece interface, namely complex loading conditions. Complex loading conditions have been widely experienced by interfacial elements during metal forming processes [17–20]. It has been found that over 99% of elements experience historical and spatial changes in interfacial conditions [21]. Protrusion features on the tool, such as draw beads and corner radii, are likely to generate higher contact pressures during the forming process than those of flat areas, such as the flange and side wall. As the forming process proceeds, the deformation and strain hardening of the workpiece may also result in a redistribution of local pressure and finally generate

a spatial distribution of the contact pressure. The sliding distance itself is a historical parameter that indicates the accumulation of the displacement between the workpiece and tool during a forming process. Instead of punch displacement, the material flow is also determined by the geometry of tool and COF, and thus makes it a spatial parameter. As the sliding speed is the derivation of the sliding distance, it is not only decided by punch speed but also inherits the historical and spatial dependency, where it varies at different locations during the forming process. The variations of contact pressure and sliding distance will further lead to the variation of interfacial temperature, as the interfacial heat transfer is highly dependent on pressure and duration of contact.

Hot stamping and hot forging processes are representative forming processes, which have been shown in Fig. 1, to demonstrate this complex loading feature. Figure 1 demonstrates how contact conditions, such as interfacial temperature, contact pressure, and relative sliding speed (shown by different colours), evolve as the function of normalized forming time. The contact condition data of every element and every stage of the forming process have been extracted from the experimentally verified simulations of hot stamping and hot forging processes to ensure the accuracy and robustness of the collected data. Normalized forming time is calculated by the ratio of current forming step and total forming step. Each ring represents a specific forming time, i.e., normalized forming time increases from 0 to 1 from the inner ring to outer ring, indicating the progress of the forming process. Each radius represents an individual element at the tool–workpiece interface. Therefore, by analyzing the information demonstrated by Fig. 1, the maximum changing and changing rate of contact conditions have been figured out and demonstrated in the table in Fig. 1. It is essential to consider and include the effects of complex loading conditions in the description of transient tribological behaviour.

The accurate representation of tribological boundary conditions is crucial for analysis and optimization for metal forming processes. But constant friction values are usually assigned to represent this highly transient interfacial condition, which would introduce deviations in the prediction. Therefore, to overview and recognize the contemporary understanding of transient tribological phenomena, the friction mechanism transition during the transient tribological phenomenon is discussed, and the relevant literatures addressing the transient phenomena under various contact scenarios are reviewed in this paper. The modelling techniques to describe the transient tribological behaviours including friction and wear are also reviewed. Subsequently, the framework of interactive friction modelling is proposed and summarized to describe and predict the transient tribological phenomenon based on the underlying friction mechanism under lubricated condition, dry sliding (metal-on-metal contact) condition, and coated system.

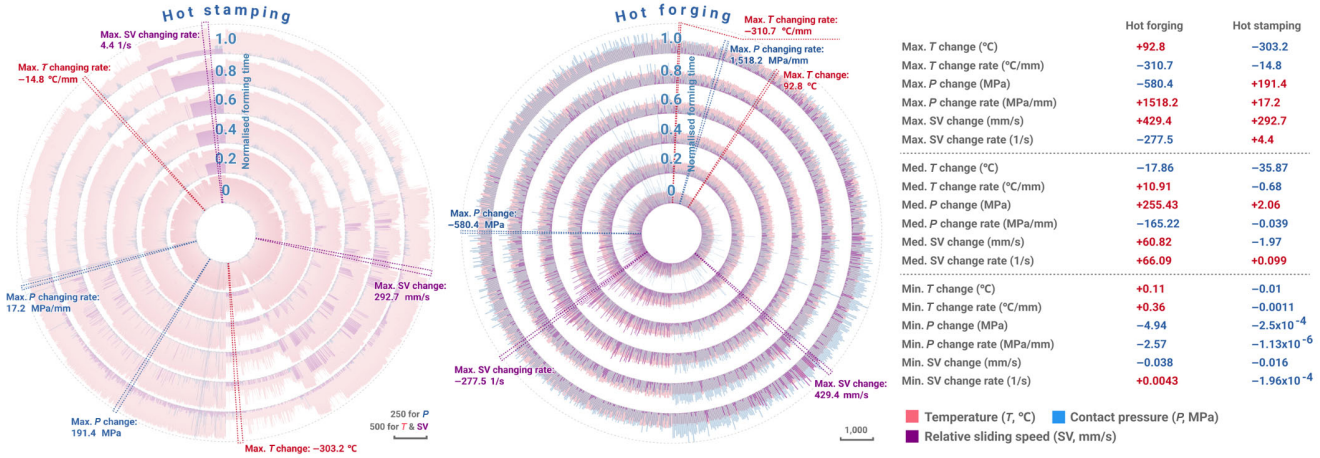

	Hot forging	Hot stamping
Max. *T* change (°C)	+92.8	−303.2
Max. *T* change rate (°C/mm)	−310.7	−14.8
Max. *P* change (MPa)	−580.4	+191.4
Max. *P* change rate (MPa/mm)	+1518.2	+17.2
Max. SV change (mm/s)	+429.4	+292.7
Max. SV change rate (1/s)	−277.5	+4.4
Med. *T* change (°C)	−17.86	−35.87
Med. *T* change rate (°C/mm)	+10.91	−0.68
Med. *P* change (MPa)	+255.43	+2.06
Med. *P* change rate (MPa/mm)	−165.22	−0.039
Med. SV change (mm/s)	+60.82	−1.97
Med. SV change rate (1/s)	+66.09	+0.099
Min. *T* change (°C)	+0.11	−0.01
Min. *T* change rate (°C/mm)	+0.36	−0.0011
Min. *P* change (MPa)	−4.94	-2.5×10^{-4}
Min. *P* change rate (MPa/mm)	−2.57	-1.13×10^{-6}
Min. SV change (mm/s)	−0.038	−0.016
Min. SV change rate (1/s)	+0.0043	-1.96×10^{-4}

Fig. 1 Complex loading conditions during hot stamping and hot forging processes: changing contact conditions (interfacial temperature, contact pressure, and relative sliding speed) vs. normalized forming time. Note: Max., Med., and Min. here represent maximum, median, and minimum, respectively.

2 Friction mechanism transition-induced transient tribological phenomena

2.1 Friction mechanism transition under lubricated contact and lubricant breakdown

Lubricant breakdown is caused by a shortage of entrapped lubricant at the contact interface, where the entrapped film thickness reduces to a certain value, which can be affected by contact conditions, operation parameters, and lubricant properties (including lubricant viscosity, η and dry matter fraction). The entrapped lubricant film reduction can be caused by a variety of reasons, such as extreme contact conditions and required load-carrying capacity [22, 23], transfer of lubricant to a newly emerged interface [24], non-uniform load distribution [17], and consumption due to chemical reaction or escaping from the interface [25, 26]. With the thinning of the lubricant film, the friction mechanism transitions from full film lubrication (i.e., hydrodynamic and elasto-hydrodynamic lubrication) occur, where the contacting surfaces are separated or protected by thick film and few asperity contacts, to boundary lubrication and finally dry sliding condition, where direct metal-on-metal contact between the mating surfaces occurs, resulting in severe scratches leading to poor component surface quality and galling on the tool, causing friction to increase [2, 4, 20, 27–29], as shown in Fig. 2.

The lubrication regime can be classified into three general conditions, as shown below, using the lambda ratio, λ, which is the ratio of mean film thickness and standard deviation of asperity heights of the two surfaces [10, 30]. The variations of these factors will lead to the transition of the lubrication regimes and simultaneously influence the friction and wear conditions.

1) Hydrodynamic or elasto-hydrodynamic lubrication ($\lambda > 5$; typical thickness: 1–100 μm)

2) Mixed lubrication ($1 < \lambda < 5$; typical thickness: 0.05–1 μm)

3) Boundary lubrication ($\lambda < 1$; typical thickness: < 0.05 μm)

The Stribeck curve [10, 27], as shown in Fig. 3, connects the lubrication mechanism transition with the variation of COF under various contact conditions and lubricant properties. The effects of these influencing

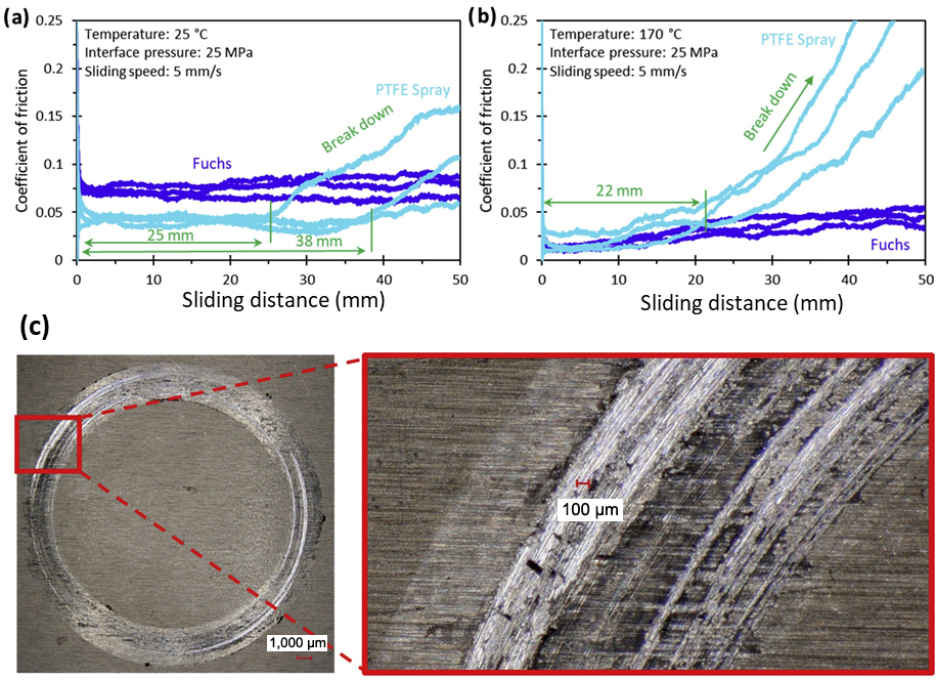

Fig. 2 Transient behaviours and lubricant breakdown phenomena: COF evolution vs. sliding distance under (a) room temperature (25 °C) and (b) elevated temperature (170 °C) with different lubricants, i.e., polytetrafluoroethylene (PTFE) spray and Fuchs, applied. (c) Observation of surface topography of wear track on the 7-series aluminium alloy specimen after twist compression tests using PTFE spray, showing severe scratching. Reproduced with permission from Ref. [4], © Elsevier B.V. 2021.

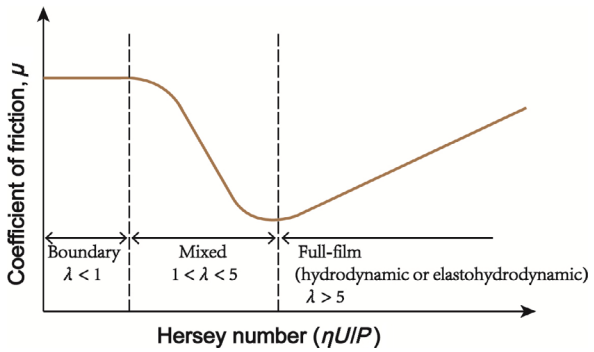

Fig. 3 Schematic diagram of Stribeck curve: relation between μ and $\frac{\eta U}{P}$. Reproduced with permission from Ref. [27], © John Wiley & Sons, Ltd 2013.

factors are described by the Hersey number, $\frac{\eta U}{P}$, where η is the lubricant viscosity, U is the sliding speed, and P is the average contact pressure. The decrease of contact pressure reduces the amount of lubricant forced out of the interface, and the increase of the sliding speed enhances the hydrodynamic effect of lubricant, both of which will lead to an increase of the lubricant film thickness, h. Direct contact between surface asperities and plastic deformation will then be alleviated, resulting in decreased friction values. The decrease of friction slows down and may reach its minimum value as the lubrication regime transitions to the full-film lubrication condition due to the increase of shear stress among the layers of thick lubricant film. It was found that the prediction of the thinning trend of the lubricant film by $\frac{\eta U}{P}$ had wide engineering applications including mechanical systems and metal working processes [31, 32].

In mechanical systems where lubricant can be replenished by the oil bath, ideal separation of contact surfaces by the hydrodynamic film can be achieved, presenting a low friction value and little wear due to relative movement. However, in metal working processes, severe contact conditions such as high contact pressure and interfacial temperature prevail at the tool–workpiece interface. The uneven distribution of contact conditions such as pressure, relative sliding distance, L, and temperature will make it difficult to control the transportation and flow of lubricant. Moreover, there is starvation of lubricant, where it cannot be replenished after the process initiates. Therefore, it is difficult to maintain sufficient lubricity under these circumstances, and there may be considerable levels of non-hydrodynamic lubrication in some tribologically-harsh location or stage, e.g., mixed or boundary lubrication and even lubricant breakdown that results in galling and abrasive wear on the tooling and formed component, even if an adequate amount of lubricant applied at the tool–workpiece interface [11, 33].

Complex loading conditions widely experienced by the interfacial elements during metal forming processes would influence physical properties and mechano-chemical behaviours of the entrapped lubricants [17, 34, 35]. Figure 4 demonstrates the evolutionary lubricant behaviours and breakdown under changing contact conditions and elevated tooling temperature scenarios. In the starving lubrication conditions, increasing contact load, W and decreasing η due to elevated temperature would result in a reduced film thickness, and thus an earlier breakdown phenomenon [11, 22, 36]. The effect of the sliding speed was found to be dependent on the speed range and might present contrasting results on the lubricant breakdown phenomenon, either increasing or decreasing the breakdown distance [22, 37]. It has been found that both the single-phase (liquid) and two-phase (liquid–solid) lubricants present a significant response of friction evolution and transient breakdown behaviours to the changing of contact conditions, which can be attributed to the combined effects of physical diminution and chemical decomposition [3, 38, 39].

2.2 Friction mechanism transition in metal-on-metal contact and galling phenomenon

Metal-on-metal contact means that no lubricant is applied between or on the contact pairs. The transient tribological phenomenon in metal-on-metal contact is mainly caused by abrasive/adhesive wear, namely galling, at the contact interface, where the initial mating contact between the tool and workpiece materials gradually transforms to the self-contact between the workpiece and transfer layer. The friction mechanism for galling can be classified into two sequential processes: (1) the wear (detachment) process and (2) the transfer process.

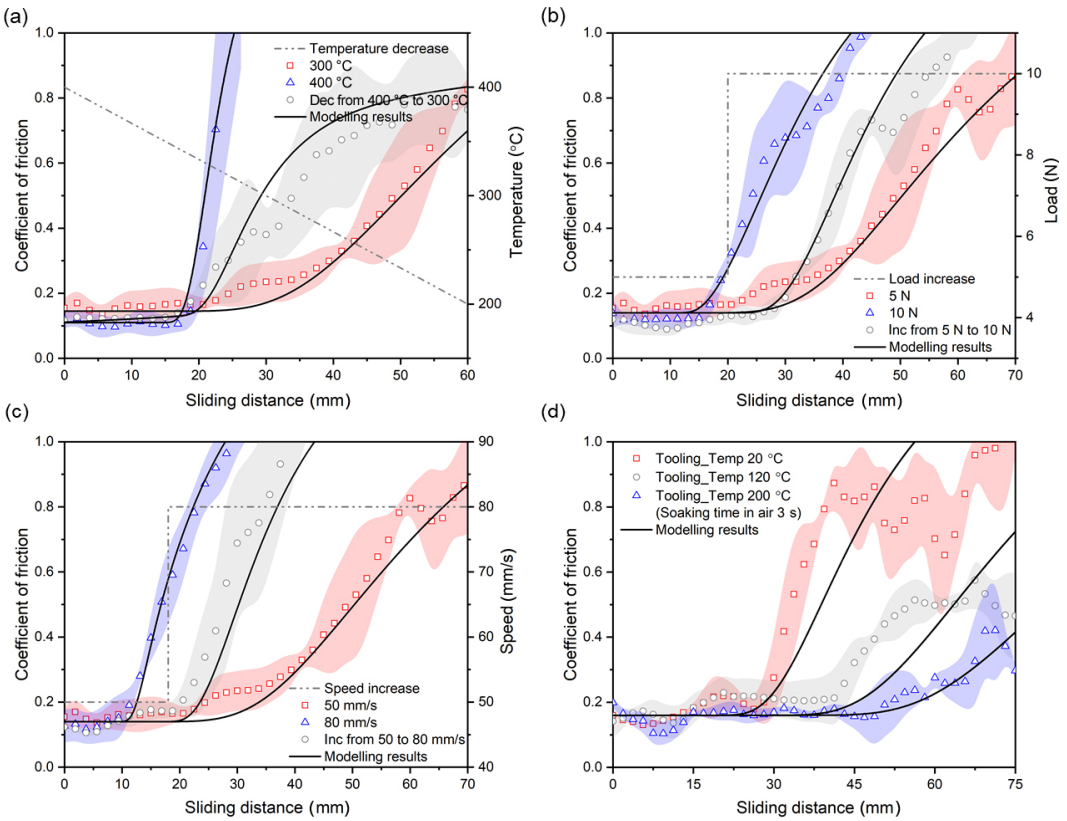

Fig. 4 Transient lubricant behaviours under complex loading conditions featuring abrupt temperature, load, and speed changes and elevated tooling temperatures. Dec and Inc represents decrease and increase, respectively. Reproduced with permission from Ref. [3] for (a–c), © The author(s) 2021; Ref. [40] for (d), © the author(s) 2022.

2.2.1 *Wear (detachment) process*

The wear process is the origin of galling as the source of the transfer material and has been identified from the original contact pairs [41, 42]. The adhesive wear mechanism has been well reviewed in Refs. [1, 10, 27, 30, 43, 44], in which Holm–Archard's and Suh's theories [43, 44] are the most influential and well accepted.

The Holm–Archard model (Eq. (1)) and its modifications [17, 27, 44] provide the basic linear relations between the factors.

$$V = \frac{kWx}{H} \tag{1}$$

where V is the wear volume, k is the wear coefficient, W is the contact load, x is the sliding distance, and H is the hardness of the soft material. In this model, increasing the contact load and sliding distance will increase the wear volume, whereas the increase of H will decrease the wear volume. Most of the material follows the trend of wear volume predicted by this model, although a more complex relation between the contact load and material hardness on the wear volume was widely observed in sliding contact.

Suh's delamination adhesive wear theory [43] explains the deformation and detachment mechanism inside soft materials. It states that large plastic strains are developed inside the workpiece and result in cracks and void nucleation in the deformation layers, which causes the generation of lathy wear particles. On a macro-scale, the increasing contact load and L can lead to the increase of the critical depth of the delamination layer. The metallurgical structure is considered in this theory but is difficult to qualitatively measure [45].

Moreover, both the Holm–Archard model [44] and Suh's delamination wear theory [43] neglect the built-up of the tribo-layer and the role of wear particles in their treatment of adhesive wear [42, 45], which have been found to form a running-in state during sliding. In metal forming processes, considerable

forming cycles occur in the running-in state, and thus its effect cannot be ignored. The study of Burwell and Strang [46] examined the running-in of wear evolutions. It was found that at the initial stage, wear increased in a nonlinear fashion due to transfer layer formation as a function of sliding distance. As shown in Fig. 5, in the running-in state, the increase of wear volume gradually slows down corresponding to the decrease of wear rate. In the steady state, the wear volume exhibits a linear relation with the sliding distance, namely a constant wear rate, which can be explained by static wear models.

2.2.2 *Transfer process*

The detached materials may transfer to the counterpart by direct and indirect transfer mechanisms. The direct transfer mechanism was proposed by Bowden and Tabor [11], where the asperities of the workpiece can directly adhere to the counterpart by mechanical and chemical bonding. In this situation, the shear strength generated at the interface is smaller than the stress inside the workpiece material, and the asperity breaks and transfer occur during sliding. Rabinowicz [47] stated a similar explanation where an adhesive junction has been formed between workpiece and tool surfaces; the junction area is likely to break inside the softer material, which generates the least resistance.

The indirect transfer mechanisms were developed by recognizing the important role of free wear particles and their effect on the tribo-system. In this case, they may freely exist at the contact interface and transfer to the counterpart with the help of external forces during sliding [48, 49]. Otherwise, the wear particles may finally be ejected. On the counterpart, the transferred wear particles may also back transfer to the original bulk material [42, 45, 50–52].

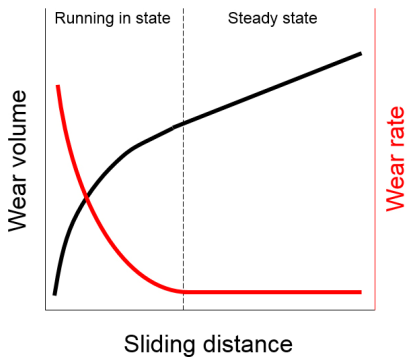

Fig. 5 Typical relation of wear volume and wear rate vs. sliding distance with transition from running-in to steady state in adhesive wear tribo-system.

The transfer process is triggered by both mechanical and chemical resistance. Mechanically, the tool surface condition is of great importance in the initial transfer process. In the wear process, in general, a certain range of the surface roughness increases the wear rate; in the transfer process, the rough surface triggers the transfer process by entrapping wear particles. In the work of Groche and Köhler [53], the cross-sectional images showed that aluminium transfer lumps were likely formed at the spheroidal graphite defects on the cast iron surface with protruding features that activate aluminium transfer. Schedin [41] reported that in sheet metal forming, the tool surface defects were the initiation sites for the material transfer. Lumps, which were observed as the individual components of the transfer layer, were built up during successive forming operations. Olsson et al. [54] carried out a similar study by a punching test between stainless sheet and American Iron and Steel Institute (AISI) M3:2. The tests showed that the initial pick-up of the workpiece filled the surface texture of the punch consisting of microscopic valleys. Hanson et al. [55] further examined the roughness effect on workpiece transfer of powder metallurgical tool steel against an austenitic stainless steel and aluminium alloy. A general conclusion was given that the risk of workpiece adhesion and transfer increased with the roughness of the tool material; however, it was still largely affected by the workpiece material and their oxidation process. Also, many patterns designed at the contact with high surface roughness can also reduce material transfer by storing wear particles [11].

Chemically, the transfer process is affected by material pairs as well as the tribo-materials that are generated by the mechanical/chemical reaction. Many commonly formed workpiece materials were reported causing galling on tool steel used in metal forming, including carbon steel [41, 56, 57], stainless steel [55, 58], and aluminium alloy [41, 55, 59–61]. According to Ref. [62], the possibility of galling between contact pairs can be explained by the influence of metallurgical compatibility, which was the degree of intrinsic attraction of the atoms between the contacting metals. High metallurgical compatibility indicated high possibility of forming strong metallic bonding.

Bhushan [27] stated that when a high contact load was applied to soft metals such as aluminium and copper, plastic deformation occurred at the contact region that led to small separations and formation of metallic bonds between the workpiece and tool. Dwivedi [51] made a similar conclusion that the actual contact area increased due to the deformation of surface asperities under an external contact load, which resulted in increased metallic intimacy.

2.3 Interaction between friction and wear

It is well observed that galling leads to transient tribological phenomena of both friction and wear at the contact. With the generation and build-up of a transfer layer from the running-in state to the steady state, the friction mechanism transitions from the original contact pair to the transfer layer contact result in high adhesion and mechanical resistance, and thus increased friction value. The roles, i.e., (1) transmitting tangential force, (2) triggering further wear and transfer, and (3) accommodating velocity difference, are played by the transfer layer and wear particles (third body) instead of the original contact pair.

As both the variations of friction and wear are related to the formation of the transfer layer, an interaction between them is formed, which has been predicted and observed in the literature. The third body theory was developed to provide a global approach to studying the galling phenomenon by focusing on the role of the interface on friction and wear. Godet [48] defined the third body by two senses. In a material sense, the third body is a zone, which exhibits a marked change in composition from the original contact pair, i.e., first body. In a kinematic sense, it could be defined as the thickness, across which the difference in velocity between solids is accommodated. The third body theory provides a global view of the whole tribo-system including the original contact pair (first body) and the generated transfer layer and wear particles at the interface (third body), thus making it a powerful approach to analyzing the adhesive wear tribo-system [63–66].

Hu et al. [67] studied the interaction between friction and wear by conducting a pin-on-disc test between the contact pair of AA6082 and cast iron G3500. Three different contact loads (2, 5, and 10 N) were used. It was found that the COF at the steady state was independent of the contact load in the test pressure range (0.64–3.18 MPa). Under different loads, the COF began at an initial value of 0.18 and increased to a constant value of 0.55. With the transfer layer gradually forming on the cast iron surface, the increase of COF and corresponding decrease of wear rate were observed. Further tests were conducted to investigate the effect of complex loading conditions, such as rapid load change, on the formation of transfer layer and galling behaviours [18], as shown in Fig. 6. It was found that the formation rate was highly dependent on the contact pressure, indicating much faster evolutions of both the COF and galling area to the saturated condition when the contact load increased from 2 to 10 N. A new phenomenon when the load decreased from 10 to 2 N was that although the COF value monotonously increased to the high plateau before the equilibrium was reached, there was a period of self-healing for the material transfer formation, demonstrating a decrease of the galling area due to secondary transfer and back transfer mechanisms.

Although anti-galling coatings are introduced with the purpose of separating the original contact pairs and could partly reduce galling, it is found that the galling formation process also widely exists in the coating system by similar mechanisms with tool steel, and there is a high level of combination between adhesive and abrasive wear in this galling phenomenon. Heinrichs et al. [60] conducted the *in-situ* experiments of sliding contact by AA6082 against diamond like carbon (DLC) coating and tool steel. Immediate pick-up of aluminium has been found in AA6082 against tool steel, compared to a slower build-up process of aluminium transfer layer in AA6082 against DLC. The transient COF value was found to be highly influenced by the scratch damage on the polished coating through the complex microscale procedure of primary, secondary, and damage-induced transfer [68]. De Rooij and Schipper [69] studied the severity of galling as a function of tool roughness for DLC coating against AA6016 T4. It was clear that lower surface roughness reduced material transfer. Also, it had been noticed that the transition from low material transfer to high material transfer occurred within a narrow range of surface roughness values. Hu et al. [70]

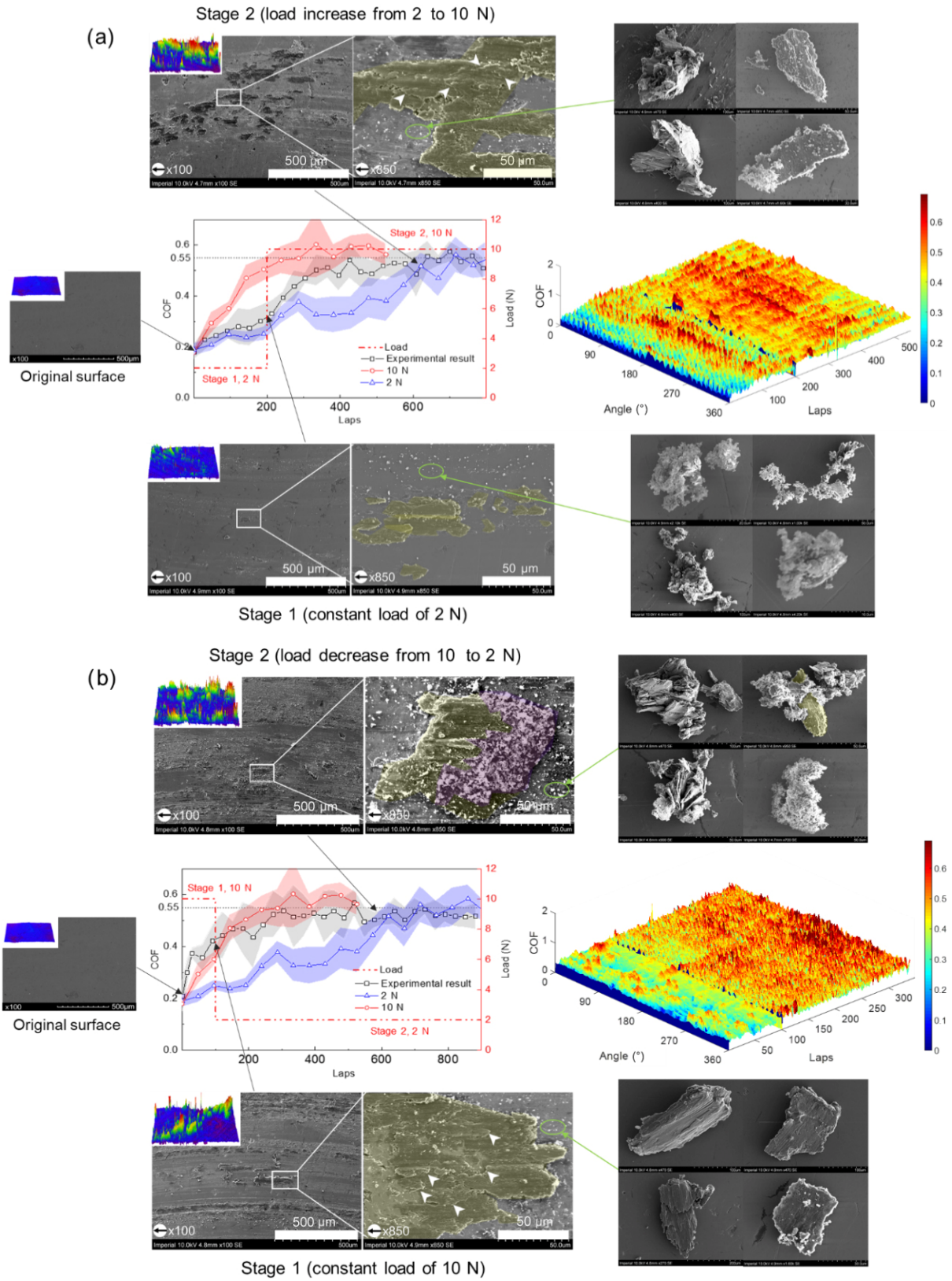

Fig. 6 Transient tribological phenomena: evolutionary friction values and interaction with surface morphologies (the galling area) under complex loading conditions in dry-sliding contact of (a) load increase and (b) load decrease. Reproduced with permission from Ref. [18], © The author(s) 2021.

examined the galling phenomenon between AA6082 against coatings of CrN and AlCrN. The primary, secondary, and damage-activated transfer were observed in these coating systems, which were triggered by the minor coating defects. Dong et al. [71] studied the anti-galling property of cathodic arc physical vapor deposition (CAPVD) WC:C coated tool against AA6082 in a U-shape bending test, as shown in Fig. 7. It showed that the WC:C coating had a much lower adhesion rate compared to the uncoated G3500 tool steel. The COF evolution of WC:C against aluminium was relatively flat, which indicates that both low severity and rapid saturation of galling were formed at the contact. An interesting dynamic COF recession phenomenon over time was observed in the WC:C coated system, which resulted from the self-passivation of free C-bonds on the coating film and absorbance of hydrogen molecule from the contact interface [71]. Apart from coatings on the tool material, coated workpiece is also utilized in some forming processes. In the direct press hardening process of Al–Si coated high-speed steel (HSS), the transient tribological behaviours were found to be determined by the morphology change and adhesive/abrasive wear of the forming tool occurred during the consecutive strip drawing [5]. Dominant wear mechanisms switched from abrasive to adhesive wear as the temperature decreased, which demonstrated an inverse trend compared with the uncoated sliding system.

The wear mechanism of galling is a combination of abrasion and adhesion. With the formation of transfer layer, wear mechanisms that were generated between the asperities of the workpiece and coated tool are partly replaced by cohesion (or self-adhesion) and abrasion between the workpiece and soft transfer layer. The tribo-system tends towards an equilibrium with active self-mating by flatting and polishing, and a transition from severe wear to mild wear occurs. This transition largely reduces the wear rate [45, 57, 58, 60, 72] to a stable value, and thus slows down the increase of wear volume to a linear relation that can be predicted by the Holm–Archard equation [46].

2.4 Friction mechanism transition in coating system and coating breakdown

When the counterpart material is much harder than the coating, and little adhesion friction exists at the contact interface, the transient friction evolution in the coating system is mainly attributed to abrasive wear of the coated material, e.g., coating breakdown and friction mechanism transition from ploughing of hard asperities to ploughing of entrapped large wear particles.

Ma et al. [8] investigated the friction evolution between WC–6% Co ball and TiN coated bearing steel GCr15 and the surface topography of the sliding wear on the coated counterpart after a series of different sliding distances, and found that the continuous sliding can be classified into three stages according to

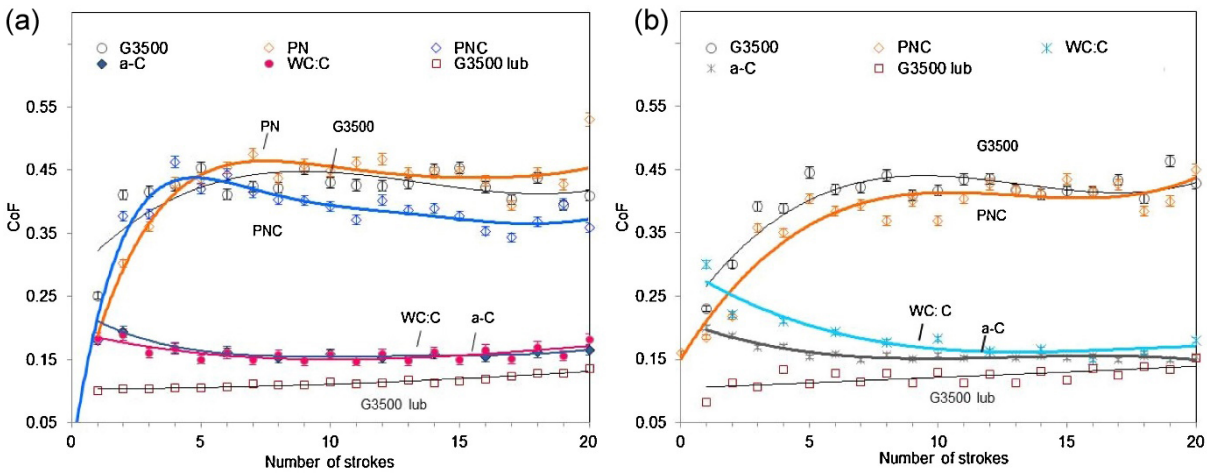

Fig. 7 Transient tribological phenomena and evolution of COF vs. number of strokes under different pressures: (a) 1.8 MPa and (b) 0.07 MPa with coated and uncoated tooling during U-shape bending of AA6082. Note: a-C here represents amorphous carbon. Reproduced with permission from Ref. [71], © Published by Elsevier B.V. 2016.

different friction mechanisms and wear behaviours, as shown in Fig. 8. The friction force mainly stems from ploughing of hard asperities, and the adhesion force is negligible between the ball and the coating [73] at room temperature in the initial low friction stage. An increased friction value is observed due to the mechanism transition to ploughing of large number and size wear particles after localized coating spallation, and it finally reaches a high plateau after complete coating breakdown and direct contact between GCr15 (substrate material) and WC ball.

There is a highly interactive relation between friction and abrasive wear in the coated system, especially when the coating breakdown initiates. Friction values begin to increase rapidly due to accumulation of hard wear particles in size and volume, and thus increased plowing forces. This will in turn accelerate the coating spallation and generation of wear particles as the shear forces increase due to increased friction. This interaction will finally lead to complete coating removal and direct contact between the substrate material and its counterpart.

A comprehensive understanding of the underlying mechanisms that drive the transient tribological phenomena at the tool–workpiece interface is essential for the establishment of descriptive and predictive models. The friction mechanism transition has been found to be closely associated with an interactive relation between friction and wear, which can be implemented properly in the model development.

3 Modelling of transient tribological behaviours (friction and wear) in metal forming

Friction models are established to describe tribological behaviours and friction values after they have been investigated and observed through friction characterization methods. In metal forming processes, an appropriate and accurate description of friction behaviours is crucial for the reliable establishment of numerical simulations. Significant efforts have been made by researchers to propose friction models to describe the tribological phenomenon under lubricated or dry condition and predict COF values, which can be employed into finite element (FE) simulations.

Wilson et al. [74] developed friction models for cold stamping under lubricant condition with the consideration of lubricant breakdown. The friction under the full film lubrication condition was calculated by Reynolds equation [75–77], as shown in Eq. (2):

$$\frac{\partial}{\partial x}\left(\frac{h^3}{12\eta}\frac{\partial P}{\partial x}\right)=\frac{\partial}{\partial x}\left(\bar{U}h\right)+\frac{\partial h}{\partial t} \tag{2}$$

where P is the pressure, and $\bar{U}$ is the average sliding speed. The transformation of lubrication regime was determined by comparing the calculated h to the surface roughness, σ. Once h was lower than 3σ, the lubrication condition was transformed to mixed lubrication conditions, in which the frictional stress,

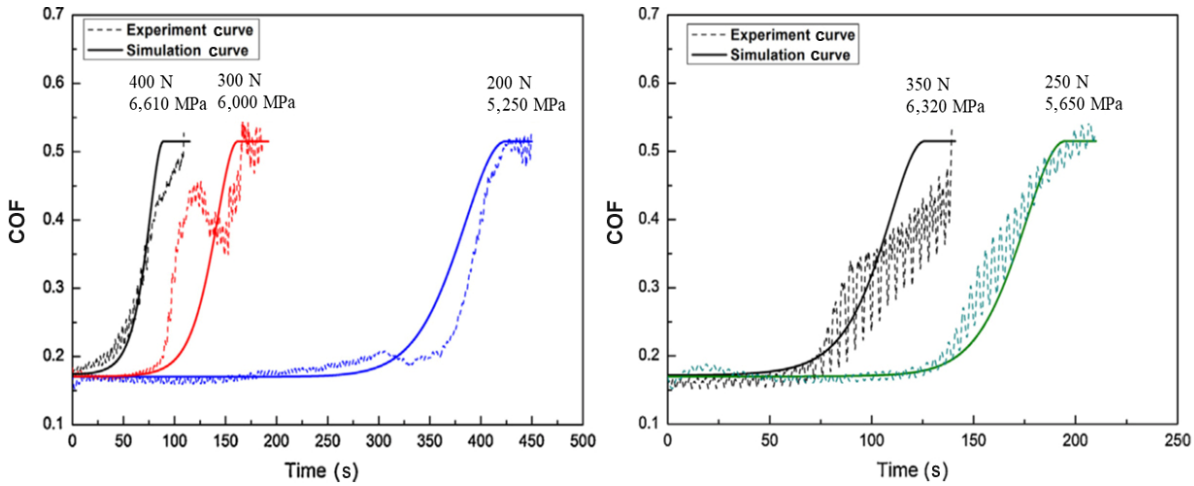

Fig. 8 Transient behaviours and coating breakdown in coated system under a series of contact load (pressure) conditions. Reproduced with permission from Ref. [8], © Elsevier B.V. 2015.

τ_f was calculated by Eq. (3):

$$\tau_f = \tau_a A + \tau_p A + \tau_h (1 - A) \tag{3}$$

where A is the frictional contact area, and τ_a, τ_p, and τ_h are the adhesion, ploughing, and hydrodynamic frictional stress components, respectively. This model was applied to model a simple stretch forming process.

Gelinck and Schipper [32] developed a model for line contact under mixed lubrication conditions. By interaction calculation and reference to the Stribeck curve, the shift between lubrication regimes, such as from boundary to elasto-hydrodynamic regime, could be predicted, and subsequently the lubrication regime can be determined for a specific contact operation. In this model, the friction force, F_f was generated by the integral of the shear stress at the asperity contact and the hydro- dynamic components (Eq. (4)):

$$F_f = 2Bb\tau_0 \operatorname{arcsinh} \frac{\eta u_{dif}}{\tau_0 h} \tag{4}$$

where B is the length of the cylinder, b is half of the contact width, τ_0 is the Eyring shear stress, and u_{dif} is the differential velocity.

A functional relationship, as shown in Eqs. (5) and (6), determining the COF between the reference forming process and a specific friction test were proposed by Groche et al. [19] based on the investigation of tribological loads, including normal pressure, σ_n, relative sliding speed, v_{rel}, surface enlargement, ψ, and interfacial temperature, T of six friction tests widely used in bulk forming processes. The model parameters (such as w, r, o, and q) were determined by optimization of deviations between different friction tests. This semi-empirical friction model was then implemented into the numerical simulation of a reference extrusion process, and a good agreement has been achieved between the experimental and numerically calculated extrusion forces before the lubricant was accumulated within the forming course.

$$\mu_{e(j)} = \mu_j K_j / K_e \tag{5}$$

$$K_{e/j} = \ln(\sigma_{n,e/j})^w \ln(v_{rel,e/j})^r \ln(\psi_{e/j})^o \ln(T_{e/j})^q \tag{6}$$

The different combination and value of e/j denote a range of frictional tests from ring compression test with boss and extrusion tests to upsetting sliding and sliding compression tests [19].

Lee et al. [78] established a friction model incorporating the effects of contact pressure, sliding velocity, and strain hardening of the deformed material on springback simulations with an oil lubricant applied. The experimental results demonstrated an increase of COF with a decrease of sliding velocity and an increase of contact pressure in the range below 10 MPa, the multiplicative relations of which were modelled by a phenomenological model, as expressed by Eq. (7):

$$\mu(v, p) = \mu_v(v)\mu_p(p) \tag{7}$$

where, v is the sliding velocity. Then, $\mu_v(v)$ (Eq. (8)) and $\mu_p(p)$ (Eq. (9)) can be characterized using the obtained experimental data.

$$\mu_v(v) = a_1 + a_2 \exp(-a_3 v) \tag{8}$$

$$\mu_p(p) = b_1(1 - \exp(-b_2 p)) \tag{9}$$

where a_1, a_2, a_3 b_1, and b_2 are model constants.

Hol et al. [79, 80] developed the multi-scale friction modelling for sheet metal forming, in which the effect of surface roughness and deformation under pressure were taken into account. In this model, the real area of contact was used to determine the influence of ploughing and adhesion effects between contacting asperities on COF. The COF was determined by the ratio of the total friction force and the total load carried by all the contact patches, as shown in Eq. (10):

$$\mu = \frac{F_W}{F_N} = \frac{\sum_{i=1}^{M_p} \mu_i(\theta_i) A_i H}{\sum_{i=1}^{M_p} A_i H} \tag{10}$$

where F_W means the total friction force, F_N means the total load carried by all contact patches, A_i is the contact area of individual patch, M_p is the number of patches, and μ_i is the individual value of COF for a single patch. μ_i was determined as a function of the attack angle, θ and the shear factor, f_c by the active contact mode including cutting, ploughing, and wear conditions, modelled by Eqs. (11)–(13):

$$\mu_{\text{cutting}} = \tan\left(\theta - \frac{1}{4}\pi + \frac{1}{2}\arccos f_{\text{c}}\right) \tag{11}$$

$$\mu_{\text{ploughing}} = \frac{B_1 \sin\theta + \cos(\arccos(f_{\text{c}} - \theta))}{B_1 \sin\theta + \sin(\arccos(f_{\text{c}} - \theta))} \tag{12}$$

$$\mu_{\text{wear}} = \frac{\left[1 - 2\sin B_2 + \left(1 - f_{\text{c}}^2\right)^{\frac{1}{2}}\right]\sin\theta + f_{\text{c}}\cos\theta}{\left[1 - 2\sin B_2 + \left(1 - f_{\text{c}}^2\right)^{\frac{1}{2}}\right]\cos\theta + f_{\text{c}}\sin\theta} \tag{13}$$

where, B_1 and B_2 are model parameters determined by the attach angle and shear factor.

A statistical approach was then adapted to transform the microscopic model to a macro-scope level, enabling the friction model to be implemented into an FE code and applied to a full-scale sheet metal forming simulation. The proposed friction model was able to predict the relation between the interfacial change and friction variation although it did not consider the galling phenomenon. This model was then further developed and expanded to include the effects of coating properties on lubricated regimes such as mixed and boundary conditions [81, 82].

A friction model was proposed to describe the decrease of τ_{f} with the increase of pressure by introducing the ratio of real contact area, α_1 and pressure in the closed pools under the liquid-lubricated condition [83]. The μ was expressed by Eq. (14) with $\alpha_1/(\alpha_1 + \beta_1)$, which represented the contribution of the nominal contact pressure made by the real contact area.

$$\mu = \frac{\tau_{\text{a}}}{p_{\text{a}}} = \frac{\alpha_1}{\alpha_1 + \beta_1}\mu_{\text{r}} \tag{14}$$

where τ_{a} and p_{a} are frictional shear stress and nominal contact pressure, respectively, μ_{r} is the friction value measured at the average pressure ratio lower than 0.5, and β_1 is a model parameter introduced under the lubricated condition. The COF decreased initially, and then became constant as the lubricant pressure reached its maximum.

The running-in state that was caused by the creation of material transfer layer was the focus of Yang's adhesive wear model [84, 85]. In the running-in state, it was assumed that the wear rate in terms of L was determined by the amount of material available at the contacting junctions. The integration of wear volume is shown in Eq. (15). This model adopted the Holm–Archard equation to model the steady state, and thus the whole wear evolution could be predicted.

$$V = A(1 - \text{e}^{-BL}) \tag{15}$$

In this model, V denotes the wear volume, and B is a model constant that is determined by contact load and surface conditions.

Fillot et al. [63] developed a wear model based on the third body concept that modelled the wear volume variations from the initial running-in to the steady state. In this model, an equilibrium of the mass inside the contact is developed, as shown in Eq. (16).

$$\frac{\text{d}M_{\text{i}}}{\text{d}t} = Q_{\text{s}} - Q_{\text{w}} \tag{16}$$

where Q_{s} is the flow of third body detached from the first body, Q_{w} is the wear flow of third body ejected outside the contact, and M_{i} is the mass of third body entrapped inside of the contact. It could be seen that the wear process constituted a form of competition between Q_{s} and Q_{w}, which were modelled by Eqs. (17) and (18), respectively. This model successfully modelled the variation of the volumetric changing rate of detached, entrapped, and ejected wear particles from the initial running-in state to the steady state.

$$Q_{\text{s}} = C_{\text{s}}(M_{\text{i}}^{\max} - M_{\text{i}}) \tag{17}$$

$$Q_{\text{w}} = C_{\text{w}}(M_{\text{i}} - M_{\text{i}}^{\text{start}}) \tag{18}$$

where C_{s} and $M_{\text{i}}^{\max}$ are constants of the experiments, $M_{\text{i}}^{\text{start}}$ is the mass of third body entrapped in unevenness of the surfaces, and C_{w} is a function of ejection speed of wear particles.

Models that focused on the growth of transfer layer were also developed. Based on the experimental results of aluminium alloy–DLC contact [69], de Rooij and Schipper [86] developed a lump growth model for general macro-scale applications, which focused on modelling of the physical contact behaviours affected by the modification of asperity height distribution during the formation of material transfer layer. Instead of a continuous transfer layer, de Rooij et al. [58]

developed a material transfer model on a single asperity scale and presented the geometrical development of a single lump over time. The shape of the lump was modelled as mechanically stable, and thus could resist the forces acted on it. The orientation of the lumps and the multi-layer structure were also considered in this model.

Most modelling studies have been focused on providing an averaged friction value by considering the effects of various factors including contact conditions and process parameters, e.g., σ_n, v_{rel}, plastic deformation, surface roughness, and interfacial temperature. Some model takes the instantaneous contact conditions into account, but the evolutionary effect of contact parameters is overlooked.

4 Development of interactive friction modelling for transient tribological phenomena

The interactive modelling frame has been introduced in describing the transient tribological behaviours under various contact scenarios, e.g., lubricated contact, metal-on-metal contact, and coating system, based on the corresponding friction mechanism transition during the sliding process. The instantaneous and evolutionary friction values and the corresponding morphology change, such as the galling area, can be expressed and predicted based on its time-dependent feature. Furthermore, the effect of evolutionary history of contact conditions, e.g., complex loading conditions, on friction and wear is also incorporated in this model, which is essential to describe the transient behaviours, as mentioned in Section 1.

To describe the transient feature of the friction value, the overall COF, $\mu(t)$, is expressed as a time-dependent variable, which is comprised of two components at the contact interface, as expressed by Eq. (19):

$$\mu(t) = (1-\beta)\mu_i(t) + \beta\mu_s(t) \tag{19}$$

where $\mu_i(t)$ and $\mu_s(t)$ are the friction values at the initial low friction state and steady high plateau state, respectively. β is included to model the transition of different friction mechanisms from the initial to the steady state. When $\beta = 0$, the transition of the friction mechanism does not occur, and the mechanism for generating low F_f is dominant. While β increases to 1, the friction mechanism transition is completed, and the mechanism for a high level of friction (steady state) takes control at the interface. β also represents the interaction between friction and wear, which will be summarized in detail in different contact scenarios.

4.1 Modelling of transient behaviours under lubricated contact

The interactive modelling for the lubricated contact [2, 3, 38] addresses the transition of boundary lubrication as well as the interaction between friction and lubricant film thinning. This model incorporates the effects of interfacial temperature, contact pressure, sliding speed, relative sliding distance, and the initial lubricant amount on the COF evolution and transient lubricant behaviours, which can be applied to scenarios involving lubricant breakdown in a dynamic contact interface such as metal forming and machining, where the use of averaged constant friction values present limitations in prediction accuracy. The model is presented in Eqs. (20)–(22).

$$\beta_1(t) = \exp\left(-\left(\frac{h_t(t)}{\lambda_{1_1}}\right)^{\lambda_{1_2}}\right) \tag{20}$$

where $\beta_1(t)$ represents the area ratio between dry condition and boundary contact, which links the interaction between friction and instantaneous lubricant film thickness, $h_t(t)$. λ_{1_1} and λ_{1_2} are model parameters, which are determined by the interfacial surface roughness and lubricant properties.

The reduction of instantaneous film thickness can be modelled by Eqs. (21) and (22), which represent the consumption of liquid lubricant and solid tribo-layer, respectively. It should be noted that the solid tribo-layer is formed due to vanish of the liquid phase (carrier agent) and deposition of solid additives under elevated temperatures. Thus, Eq. (22) is applicable to the two-phase (liquid–solid) lubricant.

$$\dot{h}_1(t) = C_1\left(h_1(t)P^{k_{1_1}}v^{k_{1_2}}/\eta^{k_{1_3}}\right) + D_1(T)(h_1(t))^{k_\alpha} \tag{21}$$

$$\dot{h}_s(t) = mD_1(T)(h_1(t))^{k_\alpha} - K(T)\frac{P^{n_{s_1}} v^{n_{s_2}}}{H_c} \quad (22)$$

where $h_1(t)$ and $h_s(t)$ denote the changing rates of thickness of the residual liquid lubricant and the solid tribo-layer, respectively, k_{l_1}, k_{l_2}, and k_{l_3} are model parameters dependent on instantaneous contact conditions, $D_1(T)$ is a temperature-dependent liquid vanishing (referring to both evaporation and decomposition as it is difficult to separate these two processes at elevated temperatures) coefficient, C_1 is a model constant, and k_α is a model parameter. m is the equivalent volume fraction of solid additives, which is determined by compositions of the two-phase lubricant. $K(T)$ is a temperature-dependent wear coefficient, and n_{s_1} and n_{s_2} are model parameters. H_c is the combined hardness of the substrate and tribo-layer, which is determined based on the mechanical properties of the solid additives and the tooling temperature.

4.2 Modelling of galling phenomenon in metal-on-metal contact

Interactive friction modelling to address the interaction between friction and adhesion wear in the galling tribo-system [18, 67] is developed to model the transient evolution of friction and saturation process of the galling area, as expressed in Eqs. (23) and (24). This model demonstrates that the formation of transfer layer is a competing result of detached material from the first body into the interface and ejected material leaving the contact interface.

$$\beta_g(t) = \overline{f}(t) = \frac{f(t)}{f(t_{sat})} = b(\overline{\rho_1}(t))^{\lambda_{g1}} \quad (23)$$

$$\dot{\overline{\rho_1}}(t) = aP^{\lambda_{g2}} T^{\lambda_{g3}} v(n\dot{\overline{\rho_1}}(t) + 1 - \overline{\rho_1}(t)) \quad (24)$$

The formation rate of the normalized third body density, $\dot{\overline{\rho_1}}(t)$, represents the formation process of the material transfer layer from the clean contact ($\overline{\rho_1} = 0$) to the equilibrium state ($\overline{\rho_1} = 1$). $f(t)$, $f(t_{sat})$, and, $\overline{f}(t)$ are the instantaneous galling area, saturated galling area, and instantaneous normalized galling area, respectively, and a relation has been built between $\overline{\rho_1}(t)$ and $\overline{f}(t)$, as shown in Eq. (23). b and λ_{g1} are model parameters. The normalized galling area varies from 0 to 1, indicating the transition of the tribo-system from an initial running-in to a final steady state and the contact condition (or friction mechanism) transition from the contact between the original pairs to that between the workpiece and transfer layer, as denoted by $\beta_g(t)$. In this model, the instantaneous form of Holm–Archard equation is adopted to model the wear rate at the steady state. a, λ_{g2}, λ_{g3}, and n are model parameters.

4.3 Modelling of transient phenomenon induced by coating breakdown

In a coating system where the adhesion force and material transfer between the coating and its counterpart play a negligible role, the transient phenomenon is usually caused by abrasive wear and interaction between friction and instantaneous coating thickness, $h_c(t)$ [8], which can be described by the interactive modelling. The contact condition (or friction mechanism) at the interface transitions from the ploughing friction between the coating and counterpart to that between the substrate and counterpart when the coating is gradually worn off and coating breakdown occurs. Therefore, the ratio of friction mechanism transitions in the coated contact, β_c, in this case, can be expressed by Eq. (25):

$$\beta_c(t) = \exp\left(-\left(\lambda_{c_1} h_c(t)\right)^{\lambda_{c_2}}\right) \quad (25)$$

where λ_{c_1} and λ_{c_2} are model parameters.

The instantaneous coating thickness can be obtained by integrating a time-dependent wear rate, $\dot{h}_c(t)$, which can be expressed based on Archard's wear equation, as shown in Eq. (26).

$$\dot{h}_c(t) = \frac{KPv}{H_c} \quad (26)$$

$$H_c = H_s(T)\frac{\alpha^2 + h_c(t)\gamma^2}{\alpha + h_c(t)\gamma^2} \quad (27)$$

where K is the coefficient of wear, which is a load-dependent and temperature-dependent parameter. H_c is the combined hardness for the contact system in both equations. Tribo-layer is treated as a kind of

coating in Eq. (22), where H_s is the hardness of the substrate material, which is temperature-dependent, α is the hardness ratio between the coating and the substrate, and γ is an influential factor of $h_c(t)$.

Section 4 introduces the investigation and development of the interactive friction models for predictions of transient friction and wear evolutions under complex loading conditions in different application scenarios. Good agreements have been achieved between the modelling results and experimental results, verifying the efficiency and accuracy of the developed models in predicting the COF evolution as a function of the instantaneous contact conditions experienced in metal forming processes. This further provides the potential of utilizing the interactive friction model in the data-driven related research.

5 Conclusions

Transient tribological phenomena are widely observed during the metal forming processes, which is induced by the transition of friction mechanisms and complex loading conditions at the contact interface. Constant friction values were usually assigned or assumed as the boundary condition to simplify the simulation process, which would introduce inaccurate predictions when describing the complex and evolutionary tribological conditions during friction-sensitive forming scenarios. In addition, as friction and wear are highly interactive tribological phenomena during the forming processes, dynamic surface morphology also exists at the tool–workpiece interface, which indicates that the transient tribological conditions become a challenge for desirable component surface quality control. The aim of this paper is to review the previous work and highlight the current research focus involving transient tribological phenomena, e.g., lubricant breakdown, galling, and coating breakdown, in metal forming processes and the interactive responses between friction and wear and their contributions to the tribo-system.

In lubricant breakdown phenomenon, the thinning of lubricant film will lead to the tribo-system to transfer to the dry sliding condition, in which friction increases due to the increased percentage of dry sliding condition, and wear rate increases due to the direct metal-on-metal contact. In galling phenomenon, the built-up of transfer layer on the tool always leads to an increase of friction due to the high cohesion between the workpiece and the transfer layer and a decrease of wear rate due to the hard tool asperities covered by relatively soft transfer layer. In coating breakdown phenomenon, coating spallation due to ploughing of large-sized wear particles will further increase F_f and accelerate generation of wear particles, thus increasing the wear rate.

Although the variation of COF due to transient tribological phenomena has widely been observed in lab-scale tests, it is still hard to be implemented into an FE software. It is because the historical effect of transient behaviours under dynamic loading conditions/between different forming cycles is still unknown. And there is still no such model that addresses complex loading parameters of metal forming. The lubrication condition in metal forming is relative better understood. However, in many lubrication models for the forming process, it is still assumed that the lubrication condition is under hydrodynamic or mixed lubrication conditions, which makes the COF vary in a low range and cannot address the consequence tribological failures, e.g., galling due to lubricant breakdown.

Thus, there is an urgent requirement to develop a holistic friction model that can describe the transient tribological conditions and address the distribution of evolutionary tribological failures under a dynamic multi-cycle forming condition. Focusing on these aims, interactive friction models have been developed, and the dependency of instantaneous contact conditions and forming history has been addressed in the holistic modelling of transient tribological phenomena, which include lubricant breakdown, galling, and coating breakdown. Future research can be focused on the implementation of interactive models into an FE simulation software and the realization of predictions of transient tribological behaviours under multi-cycle loading conditions.

Acknowledgements

This project is supported by SmartForming Research Base, Imperial College London, UK. The authors would like to acknowledge the support from Schuler Pressen GmbH, Germany, and Novelis, USA.

Declaration of competing interest

The authors have no competing interests to declare that are relevant to the content of this article.

References

[1] Kato K. Wear in relation to friction—A review. *Wear* **241**(2): 151–157 (2000)

[2] Hu Y, Wang L, Politis D J, Masen M A. Development of an interactive friction model for the prediction of lubricant breakdown behaviour during sliding wear. *Tribol Int* **110**: 370–377 (2017)

[3] Yang X, Zhang L M, Politis D J, Zhang J, Gharbi M M, Leyvraz D, Wang L L. Experimental and modelling studies of the transient tribological behaviour of a two-phase lubricant under complex loading conditions. *Friction* **10**(6): 911–926 (2022)

[4] Noder J, George R, Butcher C, Worswick M J. Friction characterization and application to warm forming of a high strength 7000-series aluminum sheet. *J Mater Process Tech* **293**: 117066 (2021)

[5] Venema J, Hazrati J, Matthews D T A, Stegeman R A, van den Boogaard A H. The effects of temperature on friction and wear mechanisms during direct press hardening of Al–Si coated ultra-high strength steel. *Wear* **406–407**: 149–155 (2018)

[6] Decrozant-Triquenaux J, Pelcastre L, Courbon C, Prakash B, Hardell J. Effect of surface engineered tool steel and lubrication on aluminium transfer at high temperature. *Wear* **477**: 203879 (2021)

[7] Hu Y R, Yuan X, Ma G J, Masen M A, Wang L L. Tool-life prediction under multi-cycle loading during metal forming: A feasibility study. *Manufacturing Rev* **2**: 28 (2015)

[8] Ma G J, Wang L L, Gao H X, Zhang J, Reddyhoff T. The friction coefficient evolution of a TiN coated contact during sliding wear. *Appl Surf Sci* **345**: 109–115 (2015)

[9] Dohda K, Boher C, Rezai-Aria F, Mahayotsanun N. Tribology in metal forming at elevated temperatures. *Friction* **3**(1): 1–27 (2015)

[10] Holmberg K, Matthews A. *Coatings Tribology: Properties, Mechanisms, Techniques and Applications in Surface Engineering*. Amsterdam (the Netherlands): Elsevier Amsterdam, 2009.

[11] Bowden F P, Tabor D. *The Friction and Lubrication of Solids*. Oxford (UK): Oxford University Press, 2001.

[12] Venema J, Matthews D T A, Hazrati J, Wörmann J, van den Boogaard A H. Friction and wear mechanisms during hot stamping of AlSi coated press hardening steel. *Wear* **380–381**: 137–145 (2017)

[13] Bull S J, Rickerby D S, Jain A. The sliding wear of titanium nitride coatings. *Surf Coat Tech* **41**(3): 269–283 (1990)

[14] Holmberg K. A concept for friction mechanisms of coated surfaces. *Surf Coat Tech* **56**(1): 1–10 (1992)

[15] Hardell J, Kassfeldt E, Prakash B. Friction and wear behaviour of high strength boron steel at elevated temperatures of up to 800 °C. *Wear* **264**(9–10): 788–799 (2008)

[16] Pelcastre L, Hardell J, Prakash B. Galling mechanisms during interaction of tool steel and Al–Si coated ultra-high strength steel at elevated temperature. *Tribol Int* **67**: 263–271 (2013)

[17] Pereira M P, Yan W Y, Rolfe B F. Sliding distance, contact pressure and wear in sheet metal stamping. *Wear* **268**(11–12): 1275–1284 (2010)

[18] Yang X, Hu Y R, Zhang L M, Zheng Y, Politis D J, Liu X C, Wang L L. Experimental and modelling study of interaction between friction and galling under contact load change conditions. *Friction* **10**(3): 454–472 (2022)

[19] Groche P, Kramer P, Bay N, Christiansen P, Dubar L, Hayakawa K, Hu C, Kitamura K, Moreau P. Friction coefficients in cold forging: A global perspective. *CIRP Ann* **67**(1): 261–264 (2018)

[20] Cui S G, Zhu H T, Wan S H, Tran B, Wang L, Tieu K. Investigation of different inorganic chemical compounds as hot metal forming lubricant by pin-on-disc and hot rolling. *Tribol Int* **125**: 110–120 (2018)

[21] Yang X, Liu H L, Dhawan S, Politis D J, Zhang J E, Dini D, Hu L, Gharbi M M, Wang L L. Digitally-enhanced lubricant

evaluation scheme for hot stamping applications. *Nat Commun* **13**: 5748 (2022)

[22] Begelinger A, De Gee A W J. Failure of thin film lubrication—A detailed study of the lubricant film breakdown mechanism. *Wear* **77**(1): 57–63 (1982)

[23] Podgornik B, Kafexhiu F, Kosec T, Jerina J, Kalin M. Friction and anti-galling properties of hexagonal boron nitride (h-BN) in aluminium forming. *Wear* **388–389**: 2–8 (2017)

[24] Bay N. The state of the art in cold forging lubrication. *J Mater Process Tech* **46**(1–2): 19–40 (1994)

[25] Rao K P, Xie C L. A comparative study on the performance of boric acid with several conventional lubricants in metal forming processes. *Tribol Int* **39**(7): 663–668 (2006)

[26] Zhang J E, Ewen J P, Ueda M, Wong J S S, Spikes H A. Mechanochemistry of zinc dialkyldithiophosphate on steel surfaces under elastohydrodynamic lubrication conditions. *ACS Appl Mater Interfaces* **12**(5): 6662–6676 (2020)

[27] Bhushan B. *Introduction to Tribology*, 2nd edn. New York (USA): John Wiley & Sons, 2013.

[28] Bay N, Olsson D D, Andreasen J L. Lubricant test methods for sheet metal forming. *Tribol Int* **41**(9–10): 844–853 (2008)

[29] Xia W Z, Zhao J W, Wu H, Zhao X M, Zhang X M, Xu J Z, Jiao S H, Wang X G, Zhou C L, Jiang Z Y. Effects of oil-in-water based nanolubricant containing TiO_2 nanoparticles in hot rolling of 304 stainless steel. *J Mater Process Tech* **262**: 149–156 (2018)

[30] Wen SZ, Huang P. *Principles of Tribology*. Singapore: John Wiley & Sons (Asia) Pte Ltd. and Tsinghua University Press, 2012.

[31] Ter Haar R. Friction in sheet metal forming, the influence of (local) contact conditions and deformation. Ph.D. Thesis. Enschede (the Netherlands): Univesity of Twente, 1996.

[32] Gelinck E R M, Schipper D J. Calculation of Stribeck curves for line contacts. *Tribol Int* **33**(3–4): 175–181 (2000)

[33] Wilson W R D. Friction and lubrication in bulk metal-forming processes. *J Appl Metalworking* **1**(1): 7–19 (1978)

[34] Karbasian H, Tekkaya A E. A review on hot stamping. *J Mater Process Tech* **210**(15): 2103–2118 (2010)

[35] Wang Z, Dohda K, Haruyama Y. Effects of entraining velocity of lubricant and sliding velocity on friction behavior in stainless steel sheet rolling. *Wear* **260**(3): 249–257 (2006)

[36] Salomon G. Failure criteria in thin film lubrication—The IRG program. *Wear* **36**(1): 1–6 (1976)

[37] Czichos H. Failure criteria in thin film lubrication—The concept of a failure surface. *Tribology* **7**(1): 14–20 (1974)

[38] Yang X, Liu X C, Liu H L, Politis D J, Leyvraz D, Wang L L. Experimental and modelling study of friction evolution and lubricant breakdown behaviour under varying contact conditions in warm aluminium forming processes. *Tribol Int* **158**: 106934 (2021)

[39] Yang X, Zhang Q L, Zheng Y, Liu X C, Politis D, El Fakir O, Wang L L. Investigation of the friction coefficient evolution and lubricant breakdown behaviour of AA7075 aluminium alloy forming processes at elevated temperatures. *Int J Extrem Manuf* **3**(2): 025002 (2021)

[40] Yang X, Zhang L M, Liu H L, Politis D J, Gharbi M M, Shi H F, Wang L L. Effect of tooling temperature on the transient lubricant behavior in hot metal forming processes. *Steel Res Int* **94**(4): 2200306 (2023)

[41] Schedin E. Galling mechanisms in sheet forming operations. *Wear* **179**(1–2): 123–128 (1994)

[42] Heilmann P, Don J, Sun T C, Rigney D A, Glaeser W A. Sliding wear and transfer. *Wear* **91**(2): 171–190 (1983)

[43] Suh N P, Tabor D. Tribophysics. *J Tribol* **109**(2): 378–379 (1987)

[44] Archard J F. Contact and rubbing of flat surfaces. *J Appl Phys* **24**(8): 981–988 (1953)

[45] Deuis R L, Subramanian C, Yellup J M. Dry sliding wear of aluminium composites—A review. *Compos Sci Technol* **57**(4): 415–435 (1997)

[46] Burwell J T, Strang C D. On the empirical law of adhesive wear. *J Appl Phys* **23**(1): 18–28 (1952)

[47] Rabinowicz E. An adhesive wear model based on variations in strength values. *Wear* **63**(1): 175–181 (1980)

[48] Godet M. Third-bodies in tribology. *Wear* **136**(1): 29–45 (1990)

[49] Berthier Y. Third-body reality—Consequences and use of the third-body concept to solve friction and wear problems. In: *Wear—Materials, Mechanisms and Practice*. Stachowiak G W, Ed. Chichester (UK): John Wiley & Sons, 2005: 291–316.

[50] Riahi A R, Alpas A T. Adhesion of AA5182 aluminum sheet to DLC and TiN coatings at 25 °C and 420 °C. *Surf Coat Tech* **202**(4–7): 1055–1061 (2007)

[51] Dwivedi D K. Adhesive wear behaviour of cast aluminium–silicon alloys: Overview. *Mater Design* **31**(5): 2517–2531 (2010)

[52] Sawyer W G, Argibay N, Burris D L, Krick B A. Mechanistic studies in friction and wear of bulk materials. *Annu Rev Mater Res* **44**: 395–427 (2014)

[53] Groche P, Köhler M. Development and application of functional surfaces. *P I Mech Eng B-J Eng* **220**(1): 19–26 (2006)

[54] Olsson D D, Bay N, Andreasen J L. Analysis of pick-up development in punching. *CIRP Ann* **51**(1): 185–190 (2002)

[55] Hanson M, Hogmark S, Jacobson S. Influence from tool roughness on the risk of work material adhesion and transfer. *Mater Manuf Process* **24**(7–8): 913–917 (2009)

[56] Okonkwo P C, Kelly G, Rolfe B F, Pereira M P. The effect of sliding speed on the wear of steel–tool steel pairs. *Tribol Int* **97**: 218–227 (2016)

[57] Landheer D, Zaat J H. The mechanism of metal transfer in sliding friction. *Wear* **27**(1): 129–145 (1974)

[58] De Rooij M B, van der Linde G, Schipper D J. Modelling material transfer on a single asperity scale. *Wear* **307**(1–2): 198–208 (2013)

[59] Olsson D D, Bay N, Andreasen J L. Prediction of limits of lubrication in strip reduction testing. *CIRP Ann* **53**(1): 231–234 (2004)

[60] Heinrichs J, Olsson M, Jacobson S. Mechanisms of material transfer studied *in situ* in the SEM: Explanations to the success of DLC coated tools in aluminium forming. *Wear* **292–293**: 49–60 (2012)

[61] Heinrichs J, Jacobson S. The influence from shape and size of tool surface defects on the occurrence of galling in cold forming of aluminium. *Wear* **271**(9–10): 2517–2524 (2011)

[62] Rabinowicz E, Tanner R I. Friction and wear of materials. *J Appl Mech* **33**(2): 479 (1966)

[63] Fillot N, Iordanoff I, Berthier Y. Wear modeling and the third body concept. *Wear* **262**(7–8): 949–957 (2007)

[64] Descartes S, Berthier Y. Rheology and flows of solid third bodies: Background and application to an $MoS_{1.6}$ coating. *Wear* **252**(7–8): 546–556 (2002)

[65] Diomidis N, Mischler S. Third body effects on friction and wear during fretting of steel contacts. *Tribol Int* **44**(11): 1452–1460 (2011)

[66] Budinski K G. *Guide to Friction, Wear, and Erosion Testing*. West Conshohocken (USA): ASTM International, 2007.

[67] Hu Y, Zheng Y, Politis D J, Masen M A, Cui J, Wang L. Development of an interactive friction model to predict aluminum transfer in a pin-on-disc sliding system. *Tribol Int* **130**: 216–228 (2019)

[68] Gil I, Mendiguren J, Galdos L, Mugarra E, Saenz de Argandoña E. Influence of the pressure dependent coefficient of friction on deep drawing springback predictions. *Tribol Int* **103**: 266–273 (2016)

[69] De Rooij M B, Schipper D J. Analysis of material transfer from a soft workpiece to a hard tool: Part II—Experimental verification of the proposed lump growth model. *J Tribol* **123**(3): 474–478 (2001)

[70] Hu Y, Zheng Y, Politis D J, Wang L, Gharbi M M. Investigation of galling behaviors between an aluminum alloy and metal forming tool. In: *Advanced High Strength Steel and Press Hardening*. Zhang Y S, Ma M T, Eds. Singapore: World Scientific, 2017: 438–442.

[71] Dong Y C, Zheng K L, Fernandez J, Li X Y, Dong H S, Lin J G. Experimental investigations on hot forming of AA6082 using advanced plasma nitrocarburised and CAPVD WC:C coated tools. *J Mater Process Tech* **240**: 190–199 (2017)

[72] Amiri M, Khonsari M M. On the thermodynamics of friction and wear—A review. *Entropy* **12**(5): 1021–1049 (2010)

[73] Wu K R, Bayer R G, Engel P A, Sun D C. Wear of physical vapor deposition TiN coatings sliding against Cr–steel and WC counterbodies. *J Tribol* **120**(3): 482–488 (1998)

[74] Wilson W R D, Hsu T C, Huang X B. A realistic friction model for computer simulation of sheet metal forming processes. *J Eng Ind* **117**(2): 202–209 (1995)

[75] Hector L G, Wilson W R D. Hydrodynamic lubrication in axisymmetric stretch forming—Part 2: Experimental investigation. *J Tribol* **113**(4): 667–674 (1991)

[76] Wilson W R D, Hector L G. Hydrodynamic lubrication in axisymmetric stretch forming—Part 1: Theoretical analysis. *J Tribol* **113**(4): 659–666 (1991)

[77] Hsu T C, Wilson W R D. Refined models for hydrodynamic lubrication in axisymmetric stretch forming. *J Tribol* **116**(1): 101–109 (1994)

[78] Lee J Y, Barlat F, Lee M G. Constitutive and friction modeling for accurate springback analysis of advanced high strength steel sheets. *Int J Plasticity* **71**: 113–135 (2015)

[79] Hol J, Meinders V T, de Rooij M B, van den Boogaard A H. Multi-scale friction modeling for sheet metal forming: The boundary lubrication regime. *Tribol Int* **81**: 112–128 (2015)

[80] Hol J, Meinders V T, Geijselaers H J M, van den Boogaard A H. Multi-scale friction modeling for sheet metal forming: The mixed lubrication regime. *Tribol Int* **85**: 10–25 (2015)

[81] Shisode M, Hazrati J, Mishra T, de Rooij M, van den Boogaard T. Mixed lubrication friction model including surface texture effects for sheet metal forming. *J Mater Process Tech* **291**: 117035 (2021)

[82] Shisode M, Hazrati J, Mishra T, de Rooij M, ten Horn C, van Beeck J, van den Boogaard T. Modeling boundary friction of coated sheets in sheet metal forming. *Tribol Int* **153**: 106554 (2021)

[83] Wang Z G, Dong W Z, Osakada K. Determination of friction law in metal forming under oil-lubricated condition. *CIRP Ann* **67**(1): 257–260 (2018)

[84] Yang L J. A test methodology for the determination of wear coefficient. *Wear* **259**(7–12): 1453–1461 (2005)

[85] Yang L J. An integrated transient and steady-state adhesive wear model. *Tribol Trans* **46**(3): 369–375 (2003)

[86] De Rooij M B, Schipper D J. Analysis of material transfer from a soft workpiece to a hard tool: Part I—Lump growth model. *J Tribol* **123**(3): 469–473 (2001)

Xiao YANG. She is a research associate in the Department of Mechanical Engineering at Imperial College London, UK. She received her Ph.D. degree at Imperial College London in 2021, and her master's degree in the Institute of Forming Technology and Equipment, Shanghai Jiao Tong University, China, in 2017. Her current research focuses on friction characterisation and interfacial behaviours in hot/warm metal forming processes. Her contributions on the development of novel interactive friction theory were recognized by prestigious awards, including "The Editors' Highlights 2022" for the best papers published in *Nature Communications* and the Unwin Prize, in recognition of her excellent Ph.D. thesis "Lubricant 4.0: Digitally Enhanced Lubricant Development for Metal Forming Applications".

Heli LIU. He received his master's degree in the College of Mechanical and Vehicle Engineering, Chongqing University, China, in 2019. He subsequently joined Metal Forming and Materials Modelling Group in Imperial College London, UK, as a Ph.D. student. His current research is data science in metal forming, which focuses on developing advanced digital technologies to enable the in depth understanding of metal forming big data.

Lemeng ZHANG. She received her bachelor's degree in mechanical engineering in 2020 at University College London, UK, and her master's degree in 2021 at Imperial College London, UK. She joined the SmartForming Research Base of Metal Forming and Modelling group at the Mechanical Engineering Department, Imperial College London and is a research postgraduate in 2022. Her current research is the development of a unified precipitation kinetics model for an Al–Mg–Si alloy undergoing ultra-FAST thermo-mechanical processing.

Yiran HU. He received his Ph.D. degree in mechanical engineering from Imperial College London, UK, in 2018. He is currently working as a data engineer at Huawei Technologies Co., Ltd., China. His research interests include prognostic health management.

Denis J. POLITIS. He is a Lecturer and Head of the Manufacturing and Materials Modelling laboratory in the Department of Mechanical and Manufacturing Engineering at the University of Cyprus, Cyprus. He has more than 10 years research experience in sheet metal forming and forging technologies. He has worked on numerous research projects in collaboration with industrial companies that have been sponsored by European FP7 and H2020 grants.

Mohammad M. GHARBI. He is Sr Manager and Forging Segment Lead at Quaker Houghton, Germany. He has broad technical expertise from managing operations to negotiating complex transformation projects across all forming technologies, hot forming and forging lubricants market in Europe, North America, and Asia.

Liliang **WANG.** Head of Metal Forming and Material Modelling group (MFG) at Imperial College London. Dr Wang is the founding director of the SmartForming Research Base at Imperial College London, and his research group is the recipient of the 2022 President's Gold Medal for Outstanding Research Team. Dr Wang's major research interests include the design and development of advanced metal forming technologies and manufacturing system. His work has made fundamental contributions to the characterization and modelling of materials and interfacial behaviours of engineering materials. Particularly, Dr Wang's research has direct impacts on lightweight manufacturing, e.g., novel lightweight forming technology: FAST *(IJP, 2019, 119: 230-248)*; Data sciences in metal forming *(Nature Communications, 2022, 13: 5748, 'The Editors' Highlights 2022' for the best papers published in Nature Communications)*; Cloud-FE technologies for metal forming process design and optimization *(JMPT, 2017, 250: 228-238)*; and innovative material characterization techniques *(Additive Manufacturing 2021, 37: 101720)*. Dr Wang has authored/co-authored 120+ papers. He has 11 filed/awarded patents; 10 patents have been taken up by lightweight manufacturing industry.